J Therm Anal Calorim (2016) 126:1–7
DOI 10.1007/s10973-016-5788-9

Yttria-stabilized zirconia–alumina composite sintering temperature effect on thermal diffusivity

Kamil Dychtoń[1] · Marcin Drajewicz[1] · Maciej Pytel[1] · Paweł Rokicki[1] · Andrzej Nowotnik[1]

Received: 15 November 2015 / Accepted: 18 August 2016 / Published online: 31 August 2016

Abstract Yttria-stabilized zirconia (YSZ) is one of the most common materials used for a ceramic top coat in the thermal barrier coating (TBC). The high operating temperature used in the gas turbine engines causes the stress between the top coat and the bond coat. The stress relaxation can be assured by modifications of YSZ. Hence, studies on how to modify the chemical and phase composition of these coatings are still conducted. The laser flash analysis was used to determine the thermal diffusivity of composite mixture of 8 mol% yttria-stabilized zirconia with α-Al_2O_3 in the range of temperatures between 20 and 1100 °C. The powders were prepared with 5 and 25 mass% Al_2O_3 addition to 8YSZ. The particle size distribution was done for each powder to analyse the grain size after milling of the α-Al_2O_3 with 8YSZ in the ball mill. The density of each powder was measured in the helium pycnometer. The disc-shaped samples were produced by pressing using an isostatic press and then sintered at various temperatures: 1000, 1200, 1400 and 1600 °C.

Keywords Laser flash analysis · Al_2O_3–YSZ composite · Thermal diffusivity

Introduction

Yttria-stabilized zirconia (YSZ) is the current state-of-the-art material widely used to protect heavily loaded parts of the stationary gas turbines and the parts in hot section of aircraft engines. The most advanced protective coatings are thermal barrier coatings (TBCs) which usually are consisted of two coatings: the first one is a diffusion aluminide coating (bond coat), and the second one is an outer ceramic coating (top coat). The main role of the TBC is to provide thermal insulation of the turbine blade (made from nickel-base superalloy). Such a coating may have a lamellar or columnar structure and can be prepared by various methods, such as *air plasma spraying* (APS), *electron beam-physical vapour deposition* (EB-PVD) or *plasma spray-physical vapour deposition* (PS-PVD). Depending on its structure and thickness can reduce the substrate temperature by up to 200 °C [1–5]. Development of the gas turbine is aimed to produce engines that will be able to withstand increased turbine entry temperature (TET), well beyond 1600 °C [6–9]. The higher operating temperature in the gas turbine engines the more improvements in the TBCs development for turbine blades based on nickel superalloys [10]. Traditionally, ZrO_2 that has been partially stabilized with 8 mol% Y_2O_3 is used for TBCs. Unfortunately, YSZ coatings show insufficient phase stability and accelerated sintering at temperatures higher than 1200 °C [9]. Therefore, it is crucial to search for alternative stabilizers or alternative materials for TBCs, with improved phase stability.

At the room temperature, the structure of pure zirconia ZrO_2 is monoclinic, but in higher temperatures it undergoes monoclinic–tetragonal and tetragonal–cubic structural phase transitions (at 1167 and 2397 °C) [11]. However, the fluorite-type cubic structure of the high-temperature phase can exist at room temperature by doping lower-valent metal oxides like Y_2O_3, which is so-called yttria-stabilized zirconia (YSZ) [11]. Yttria is the most popular stabilizer used for zirconia ceramics for its excellent mechanical and wear properties and a good effect on tetragonal phase

✉ Kamil Dychtoń
kdychton@prz.edu.pl

[1] Rzeszow University of Technology, Al. Powstancow Warszawy 12, 35-959 Rzeszow, Poland

transformability [12]. Unfortunately, YSZ coatings show phase instability and accelerated sintering at temperatures higher than 1200 °C for TBCs systems. Thermal shock and failure occur during rapid cooling. The monoclinic to tetragonal phase transformation results in a volume change and from that causes high stresses [13]. Therefore, the monoclinic phase formed by phase transformation during temperature variation causes rapid spallation of the TBC. Not even a strain-tolerant, columnar microstructure can accommodate these stresses. Thermal shock resistance of cubic 8 mol% YSZ can be increased by the addition of dilute second phase [14]. That second phase can be α-Al_2O_3. Many studies have reported that Al_2O_3 addition to YSZ not only assisted sintering but also lowered the overall and grain-boundary resistivity of YSZ [15]. This mixture of YSZ and Al_2O_3 can be prepared as powder for the low-pressure plasma spraying (LPPS) or as ceramic bars for electron beam-physical vapour deposition (EB-PVD) and used for creation of top coat in TBCs system [16–18]. It is crucial to measure the thermal diffusivity of the ceramic powders to compare it with the thermal diffusivity of ceramic topcoat deposited on the surface of the turbine blades.

This study addresses how dilute second phase affects the thermal diffusivity for two-phase ceramic composites of 8 mol% YSZ with alumina oxide (α-Al_2O_3) after sintering in the range of temperature 1000–1600 °C. Experimental characterization of the thermal diffusivity for ceramics composite was performed using the laser flash method (LFA) in the range of temperatures between 20 and 1100 °C.

Experimental

In this paper, the thermal diffusivity of yttria-stabilized zirconia (YSZ) with α-Al_2O_3 composite was measured by laser flash analysis [19, 21–23]. This method is based on monitoring the temperature excursion generated on the sample back face resulting from deposition of a very short but intense laser energy pulse on rear face surface of a sample. Due to the heat loss effects—especially for high temperature—the data reduction need to be accounted [20]. This is done by the formula available in the software of LFA 447 Netzsch Instruments. The analysis of the data was done in connection with the radiation model design for the measurement of ceramic. The voltage of the laser used in the laser flash analysis was 600 V, and the pulse width was equal to 0.5 ms for all measurements. Samples which can be measured in laser flash technique need to have a disc shape. Yttria-stabilized zirconia–alumina (YSZ–Al_2O_3) composites containing 5 and 25 mass% of α-Al_2O_3 were mixed in a ball mill to ensure homogeneity. Density of ceramic composites was measured in the helium pycnometer. In this measurement, the inert gas is used as the displacement medium. The sample solid-phase volume is measured by comparison with pressure of gas in the sample chamber with the same volume of gas after discharging into a second empty chamber. Dividing the sample weight by measured volume gives the bulk density. The density was measured ten times, and average value is presented in Table 1. The flat samples were formed in the shape of cylinder with diameter equal 12.5 mm. To appropriate quantification of powder, three drops of glycerine were added before pressing. The forming of powder to the stiff and flat samples was realized in a one direction manually operated hydraulic press with a pressure force 200 kN at room temperature. Samples were sintered in, respectively, temperature 1000, 1200, 1400 and 1600 °C for 4 h with slow cooling to room temperature. Before analyses, both surfaces of samples were covered with graphite. The black coating to absorb the laser beam energy is required for the specimen which is transparent, translucent or low emissivity. The SEM microscopic investigation of pressed and sintered Al_2O_3–YSZ composites were carried out using Hitachi S3400 N scanning electron microscope equipped with X-ray energy dispersive spectrometer (EDS). The results of SEM research are presented in Figs. 7 and 8. The particle size distribution was done for powder of 5 and 25 mass% Al_2O_3–YSZ composites in the DigiSizer II and is presented in Fig. 10.

Results

The density of the 5 and 25 mass% Al_2O_3–YSZ composites is presented in Table 1. The value of the density for the 25 mass% Al_2O_3–YSZ composite is smaller than the density for the 5 mass% Al_2O_3–YSZ composite, and this shows that the ball milling was correctly carried out before

Table 1 Density of the composites measured in the pycnometer

Bulk density of powders/gcm^{-3}	5 mass% Al_2O_3–YSZ	25 mass% Al_2O_3–YSZ
Average	4.5350	3.9933
Standard deviation	0.0109	0.0106

preparing the disc-shaped samples and shows how the density of the composite is changed with addition of the Al_2O_3. The thermal diffusivity of the two types of the composite, one with 5 mass% addition of Al_2O_3 in the YSZ and the second with 25 mass% Al_2O_3 in the YSZ, is presented in Figs. 1–5.

The thermal diffusivity values for both types of composites samples sintered at the temperature 1000 °C decrease with temperature to 0.15 $mm^2\ s^{-1}$ at 700 °C. Then the values for the composite with 5 mass% Al_2O_3 start to increase to 0.18 $mm^2\ s^{-1}$; on the other hand, the values for composite with 25 mass% Al_2O_3 stayed at the same level. For the samples sintered at the temperature 1200 °C, the change of the thermal diffusivity values has different tendency than for the temperature 1000 °C. The values for the composite with 5 mass% Al_2O_3 decrease to 0.33 $mm^2\ s^{-1}$ at the temperature 600 °C and then stay at this level to 1100 °C. At the same time, the values of the thermal diffusivity for the composite with 25 mass% Al_2O_3 are equal to 0.23 $mm^2\ s^{-1}$ for whole range of the measurement temperature. For 1400 °C sintering temperature, the thermal diffusivity for 25 mass% Al_2O_3 has bigger values than for 5 mass% Al_2O_3 and this is quite different from 1000 to 1200 °C. It can be caused by the intrinsic cracks. The values of thermal diffusivity for the composite with 25 mass% Al_2O_3 decrease to 0.36 $mm^2\ s^{-1}$ at 800 °C and then insignificantly increase to 0.38 $mm^2\ s^{-1}$. The values of thermal diffusivity for the composite with 5 mass% Al_2O_3 increase from 0.23 to 0.29 $mm^2 s^{-1}$ in the whole range of measurement temperature. For 1600 °C sintering temperature, the values of thermal diffusivity for both composites have the same tendency and increase in the whole range of measurement temperature from 0.28 to 0.37 $mm^2\ s^{-1}$ for 5 mass% of Al_2O_3 and from 0.26 to 0.32 $mm^2\ s^{-1}$ for 25 mass% of Al_2O_3. In Fig. 5, all measurements are presented. The analysis for all sintering

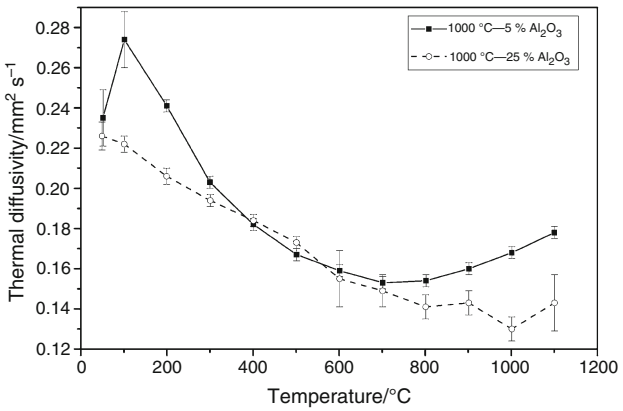

Fig. 1 Comparison of thermal diffusivity of 5 and 25 mass% Al_2O_3–YSZ composite in 1000 °C

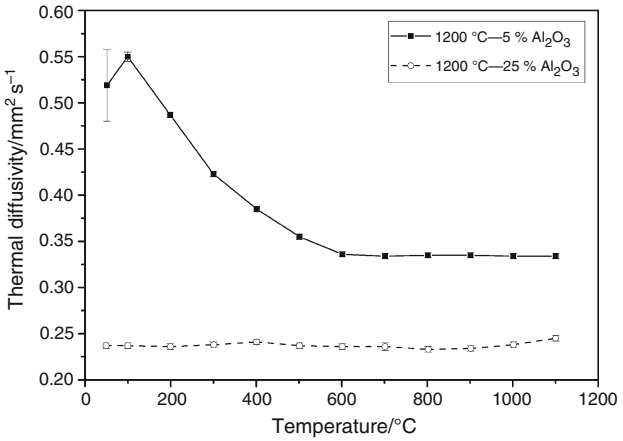

Fig. 2 Comparison of thermal diffusivity of 5 and 25 mass% Al_2O_3–YSZ composite in 1200 °C

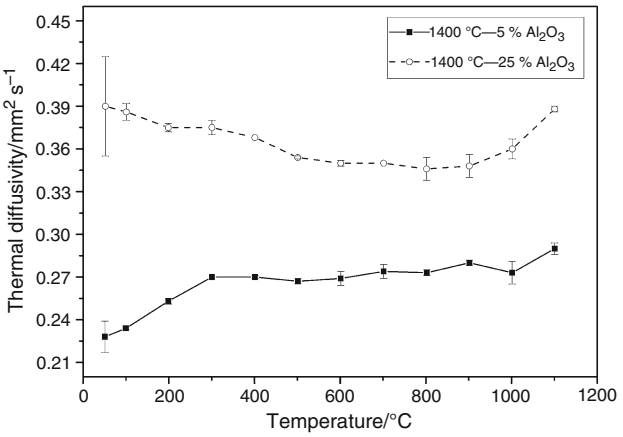

Fig. 3 Comparison of thermal diffusivity of 5 and 25 mass% Al_2O_3–YSZ composite in 1400 °C

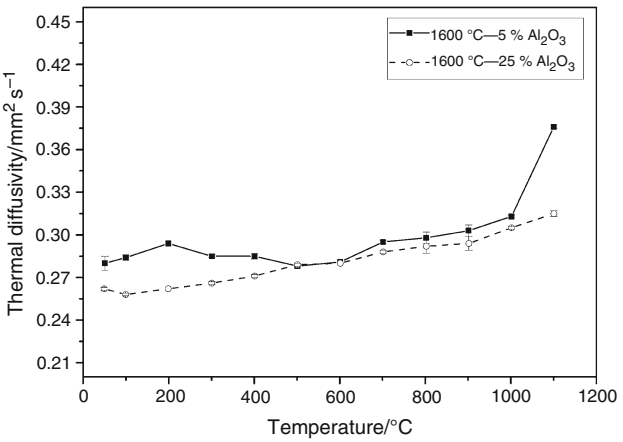

Fig. 4 Comparison of thermal diffusivity of 5 and 25 mass% Al_2O_3–YSZ composite in 1600 °C

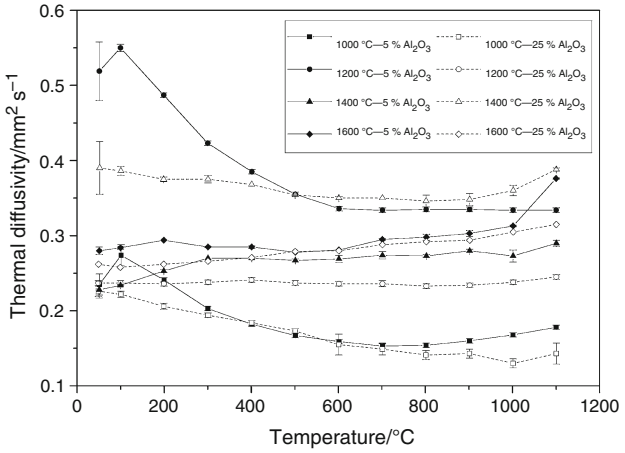

Fig. 5 Comparison of thermal diffusivity of 5 and 25 mass% Al_2O_3–YSZ composite in all temperatures

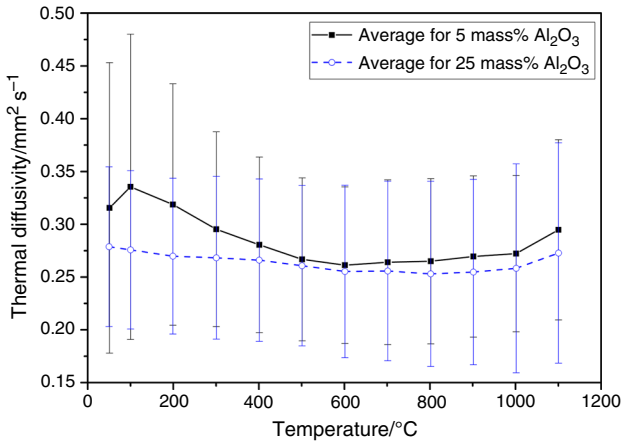

Fig. 6 Comparison of average thermal diffusivity of 5 and 25 mass% Al_2O_3–YSZ

temperatures shows that there is no significant difference in the thermal diffusivity measured by laser flash for both composites in the temperatures 1400 and 1600 °C. The considerable difference can be seen for the sintering temperatures −1000 and 1200 °C. For both composites, the thermal diffusivity in this temperature has tendency to decrease with temperature. The average thermal diffusivity for both composites is measured and presented in Fig. 6.

The SEM microscopic investigation of pressed and sintered Al_2O_3–YSZ composites was the basis for the analysis of their morphology and microstructure. The microstructure illustrates the effect of sintering temperature on morphology of the samples. It was found that the samples heated at temperatures of 1000 and 1200 °C for 4 h were not well sintered (Fig. 7a–d) and the morphology of YSZ and Al_2O_3 powder particles is angular while for the temperature of 1400 °C can be seen clearly sintering characteristics, the particles of Al_2O_3 and YSZ powders have a more rounded shape (Fig. 7e, f) than for samples sintered at 1000 and 1200 °C. The microstructure of samples sintered at a temperature of 1600 °C is more uniform and dense and is characterized by a lower porosity (Fig. 7g, h). The EDS X-ray maps show that the dispersion of Al_2O_3 powder particles is similar for all the samples at all temperatures for both 5 and 25 mass% Al_2O_3, and present are agglomerates of YSZ and Al_2O_3 (Fig. 8). Figure 9a, b illustrate the presence of the Al_2O_3 and YSZ powder particles in microstructure of Al_2O_3–YSZ composites for 25 mass% Al_2O_3 sintered at a temperature of 1000 °C and 1600 °C.

The analysis of particle size distribution is presented in Fig. 10. The volume per cent for 5 mass% Al_2O_3–YSZ composite and for 25 mass% Al_2O_3–YSZ composite is presented in Fig. 10 and shows that after milling in the powder there is non-uniform distribution of the particle diameter. This causes creation of porosity in the pressed and sintered samples and can affect the thermal diffusivity measurements of ceramics samples in the laser technique as it can be seen in Figs. 1–4.

Discussion

The analysis of thermal diffusivity of the 5 and 25 mass% Al_2O_3–YSZ composites in the temperature range 20–100 °C was presented. Figure 6 presents the average values of thermal diffusivity with standard deviation measured for both 5 and 25 mass% Al_2O_3–YSZ composites on the samples sintered in the temperatures: 1000, 1200, 1400 and 1600 °C. The average thermal diffusivity values of Al_2O_3–YSZ composite in the range of temperature 20–1100 °C show higher deviations for lower temperatures. This is due to the small amount of laser energy in comparison with heat loss effects. Akin et al. [17] show that for pure Al_2O_3 sample the displacement during sintering appears from 900 to 1300 °C and for Al_2O_3-10 mol% YSZ composites the displacement appears from 1200 to 1400 °C. This can suggest that samples sintered below 1400 °C would be unstable for measuring thermal diffusivity by laser flash technique. Schlichting et al. [12] considered the influence of porosity on thermal conductivity and showed that the increase in porosity causes the decrease in values of thermal conductivity with increasing in temperature. In this study, the effect of porosity was not considered. In this publication, the thermal diffusivity for both composites increases after 1000 °C which is shown in Fig. 6. All authors [12, 13, 17] considered thermal conductivity of Al_2O_3–YSZ composites after sintering samples in 1500 °C. The authors of this publication considered the influence of sintering temperature from 1000 to 1600 °C on thermal diffusivity measured with laser flash technique. The results showed that for both 5 and 25 mass% Al_2O_3–YSZ composites sintered in 1000 °C the thermal diffusivity

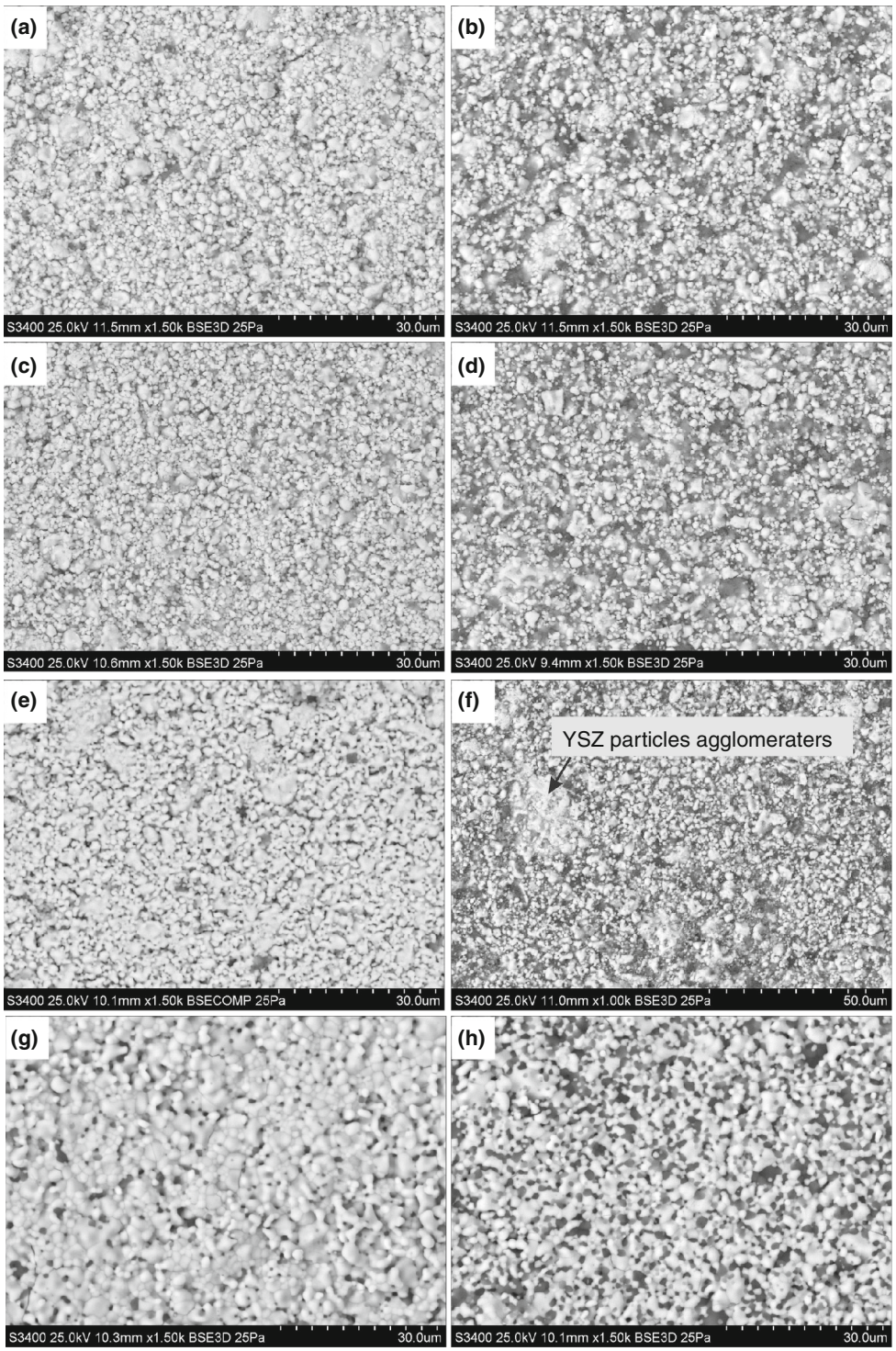

Fig. 7 SEM–BSE micrographs of sintered Al_2O_3–YSZ composites sintered at a temperature of **a** 1000 °C 5 mass% Al_2O_3; **b** 1000 °C 25 mass% Al_2O_3; **c** 1200 °C 5 mass% Al_2O_3; **d** 1200 °C 25 mass% Al_2O_3; **e** 1400 °C 5 mass% Al_2O_3; **f** 1400 °C 25 mass% Al_2O_3; **g** 1600 °C 5 mass% Al_2O_3; **h** 1600 °C 25 mass% Al_2O_3

decreases with temperature. For temperatures 1200, 1400 and 1600 °C, the thermal diffusivity decreases up to 1000 °C and then increases. This can suggest the thermal conductivity of both 5 and 25 mass% Al_2O_3–YSZ composites also increases. The large value of deviation for thermal diffusivity suggests that the laser flash analysis for ceramic powder needs broader researches. The SEM microstructure investigations showed crucial differences in morphology studies composited in the

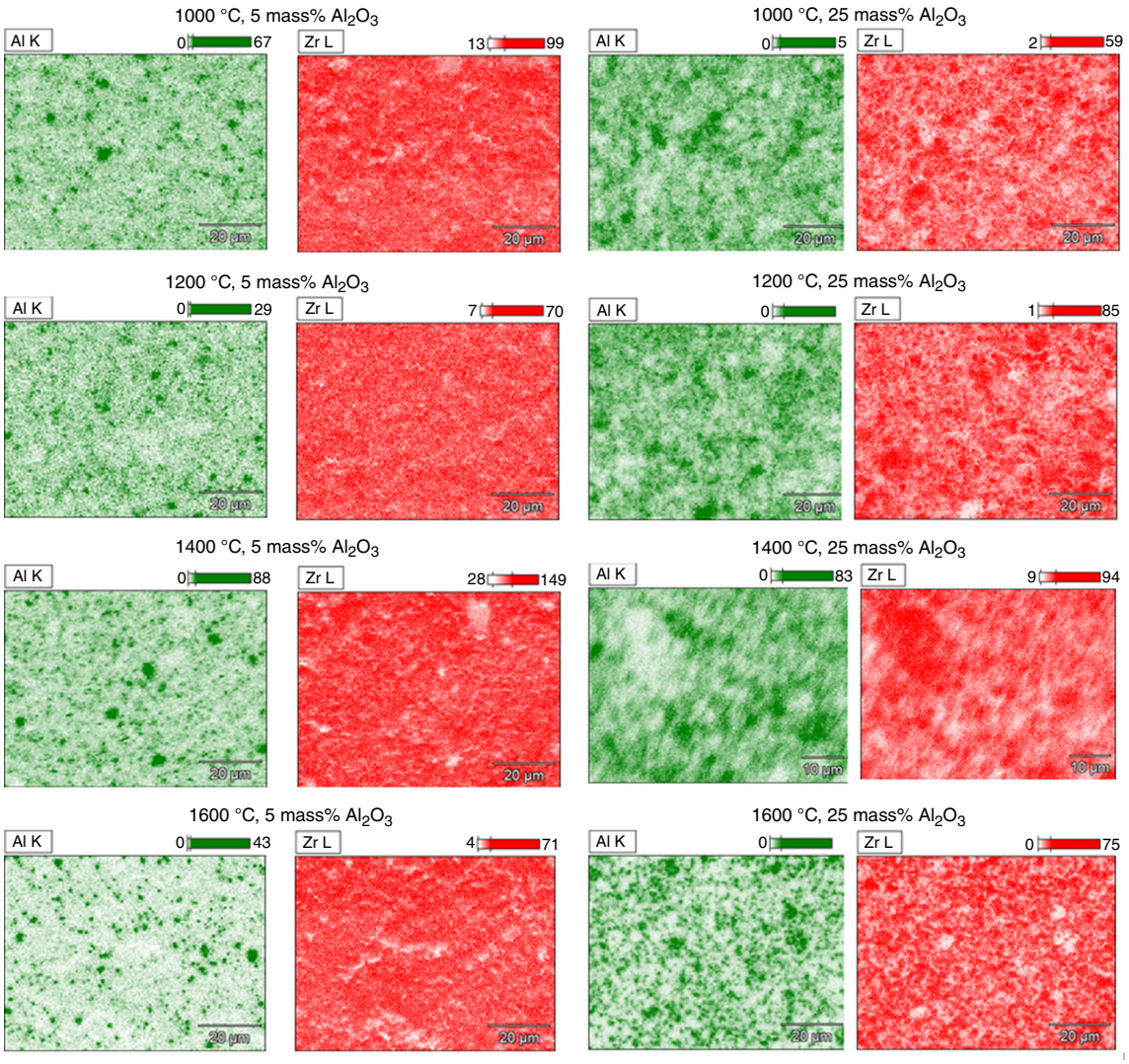

Fig. 8 Results of the EDS X-ray mapping analysis. The images show microareas of aluminium and zirconium concentrations in sintered YSZ–Al_2O_3 composites

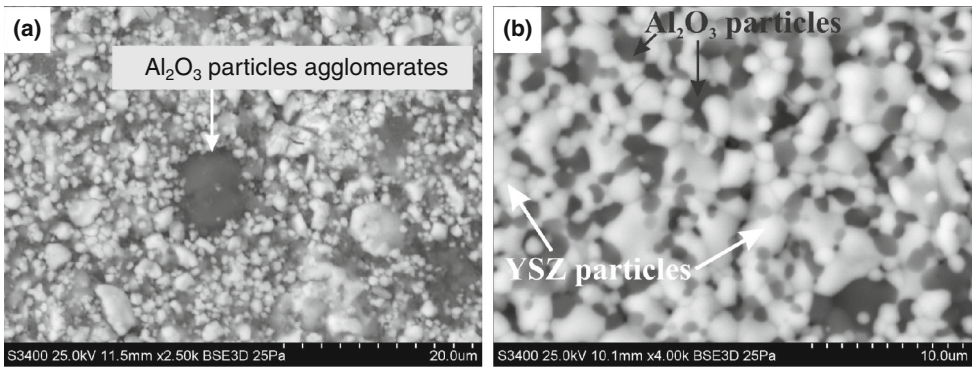

Fig. 9 SEM–BSE micrographs of morphology of Al_2O_3–YSZ composites for 25 mass% Al_2O_3 sintered at a temperature of **a** 1000 °C and **b** 1600 °C

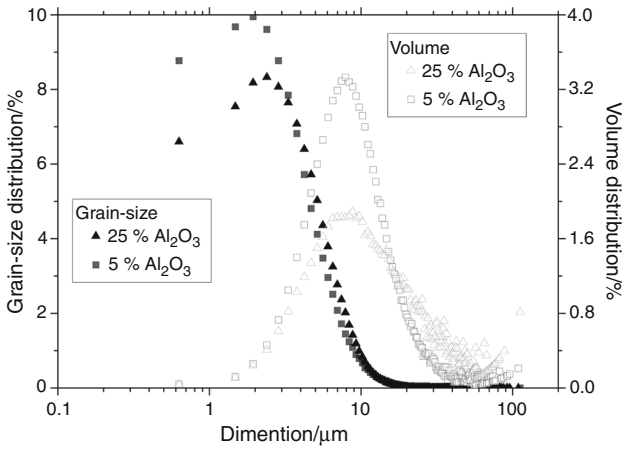

Fig. 10 Particle grain size and volume distribution for 5 and 25 mass% Al_2O_3–YSZ composite

influence of sintering temperature. The analysis of particle size distribution shows non-uniform particle diameter. This causes bigger non-stability in the laser flash measurements and can be the source of intrinsic cracks in the ceramics samples prepared for thermal diffusivity measurements. The average values of thermal diffusivity for 5 and 25 mass% Al_2O_3–YSZ composites measured by laser flash method in this paper showed differences in comparison with others values presented in literature. The Al_2O_3–YSZ composite is well known, and its thermal properties are the subject of the researches since long time. Nevertheless, the influence of each oxide's chemical composition, porosity and size of particles in the composite is still unknown. It should be noted that in present work an influence of the porosity and density of Al_2O_3–YSZ composites on their thermal conductivity and diffusivity was not taken into account and it will be the subject of further research.

References

1. Strangman TE. Thermal barrier coatings for turbine airfoils. Thin Solid Films. 1985;127:93–105.
2. Evans AG, et al. Mechanisms controlling the durability of thermal barrier coatings. Prog Mater Sci. 2001;46(46):505–53.
3. Swadźba L, Moskal G, Mendala B, Gancarczyk T. Characterisation of APS TBC system during isothermal oxidation at 1100 °C. Adv Mater Sci Eng. 2007;28(12):757–64.
4. Padture NP. Thermal barrier coatings for gas-turbine engine applications. Science. 2002;296(5566):280–4.
5. Schulz U. Microstructure and texture of EB–PVD TBCs grown under different rotation modes. Mater Sci Eng A. 2003; 360(1–2):319–29.
6. Von Niessen K, Gindrat M, Refke A. Vapor phase deposition using plasma spray-PVD^{TM}. J Therm Spray Technol. 2010; 19(1–2):502–9.
7. Góral M, Kotowski S, Nowotnik A, Pytel M, Drajewicz M, Sieniawski J. PS–PVD deposition of thermal barrier coatings. Surf Coat Technol. 2013;237:51–5.
8. Munawar AU, Schulz U, Cerri G. Microstructural evolution of GdZ and DySZ based EB–PVD TBC systems after thermal cycling at high temperaturę. J Eng Gas Turbines Power. 2013;135(10):1–6.
9. Schulz U. Phase transformation in EB–PVD yttria partially stabilized zirconia thermal barrier coatings during annealing. J Am Ceram Soc. 2000;83(4):904–10.
10. Drajewicz M, Dychton K, Goral M. Thermal properties of YSZ powders for plasma spraying. Solid State Phenom. 2015;227: 413–6.
11. Tojo T, Atake T, Mori T, Yamamura H. Excess heat capacity in yttria stabilized zirconia. J Therm Anal Calorim. 1999;57(2):447–58.
12. Schlichting KW, Padture NP, Klemens PG. Thermal conductivity of dense and porous yttria-stabilized zirconia. J Mater Sci. 2001;36(12):3003–10.
13. Angle JP, Wang Z, Dames C, Mecartney ML. Comparison of two-phase thermal conductivity models with experiments on dilute ceramic composites. J Am Ceram Soc. 2013;96(9): 2935–42.
14. Chen M, Hallstedt B, Gauckler LJ. Thermodynamic modeling of the ZrO_2–$YO_{1.5}$ system. Solid State Ion. 2004;170(3–4):255–74.
15. Ravichandran KS, An K, Dutton RE, Semiatin SL. Thermal conductivity of plasma-sprayed monolithic and multilayer coatings of alumina and yttria-stabilized zirconia. J Am Ceram Soc. 1999;82(3):673–82.
16. Hofmeister AM. Thermal diffusivity and thermal conductivity of single-crystal MgO and Al2O3 and related compounds as a function of temperature. Phys Chem Miner. 2011;41(5):361–71.
17. Akin I, Yilmaz E, Sahin F, Yucel O, Goller G. Effect of CeO2 addition on densification and microstructure of Al_2O_3–YSZ composites. Ceram Int. 2014;37(8):3273–80.
18. Hotza D, Leo A, Sunarso J, da Diniz Costa JC. Effect of Nano-Al_2O_3 addition on the densification of YSZ electrolytes. J Nano Res. 2009;9:115–22.
19. Manuelian M, Campbell R. Thermal diffusivity, specific heat, and thermal conductivity measurment using NETZSCH LFA 447 Nanoflash^{TM}. Netzsch Instrum. 2008;1–8.
20. Oksanen M, Volcan A, Fenici P. Simulations on the accuracy of laser-flash data analysis methods. Rev Prog Quant Nondestr Eval. 1996;15:549–52.
21. Parker WJ, Jenkins RJ, Butter CP, Abbot GL. Flash method of determining thermal diffusivity, heat capacity and thermal conductivity. J Appl Phys. 1961;32:1679–84.
22. Shinzato K, Baba T. A laser flash apparatus for thermal diffusivity and specific heat capacity measurements. J Therm Anal Calorim. 2001;64:413–22.
23. Gaal PS, Thermitus MA, Stroe DE. Thermal conductivity measurements using the flash method. J Therm Anal Calorim. 2004;78:185–9.